

SIMP J013656.5+093347 IS LIKELY A PLANETARY-MASS OBJECT IN THE CARINA-NEAR MOVING GROUP

JONATHAN GAGNÉ,^{1,2} JACQUELINE K. FAHERTY,³ ADAM J. BURGASSER,⁴ ÉTIENNE ARTIGAU,⁵ SANDIE BOUCHARD,⁵ LOÏC ALBERT,⁵ DAVID LAFRENIÈRE,⁵ RENÉ DOYON,⁵ AND DANIELLA C. BARDALEZ GAGLIUFFI⁶

¹*Carnegie Institution of Washington DTM, 5241 Broad Branch Road NW, Washington, DC 20015, USA*

²*NASA Sagan Fellow*

³*Department of Astrophysics, American Museum of Natural History, Central Park West at 79th St., New York, NY 10024, USA*

⁴*Center for Astrophysics and Space Sciences, 9500 Gilman Dr., Mail Code 0424, La Jolla, CA 92093, USA*

⁵*Institute for Research on Exoplanets, Université de Montréal, Département de Physique, C.P. 6128 Succ. Centre-ville, Montréal, QC H3C 3J7, Canada*

⁶*Center for Astrophysics and Space Sciences, University of California, San Diego, 9500 Gilman Dr., Mail Code 0424, La Jolla, CA 92093, USA*

(Received 2017 April 22; Revised 2017 May 2; Accepted 2017 May 3)

Submitted to ApJ Letters.

ABSTRACT

We report the discovery that the nearby (~ 6 pc) photometrically variable T2.5 dwarf SIMP J013656.5+093347 is a likely member of the ~ 200 Myr-old Carina-Near moving group with a probability of $> 99.9\%$ based on its full kinematics. Our $v \sin i$ measurement of $50.9 \pm 0.8 \text{ km s}^{-1}$ combined with the known rotation period inferred from variability measurements provide a lower limit of $1.01 \pm 0.02 R_{\text{Jup}}$ on the radius of SIMP0136+0933, an independent verification that it must be younger than ~ 950 Myr according to evolution models. We estimate a field interloper probability of 0.2% based on the density of field T0–T5 dwarfs. At the age of Carina-Near, SIMP0136+0933 has an estimated mass of $12.7 \pm 1.0 M_{\text{Jup}}$ and is predicted to have burned roughly half of its original deuterium. SIMP0136+0933 is the closest known young moving group member to the Sun, and is one of only a few known young T dwarfs, making it an important benchmark for understanding the atmospheres of young planetary-mass objects.

Keywords: stars: individual (SIMP J013656.5+093347) — brown dwarfs — stars: kinematics and dynamics — planets and satellites: atmospheres

arXiv:1705.01625v1 [astro-ph.SR] 3 May 2017

1. INTRODUCTION

Young brown dwarfs near to and below the deuterium burning mass boundary have the potential to serve as benchmarks in understanding the atmospheres and fundamental properties of gas giant exoplanets, as they share similar temperatures, surface gravities and masses (Gagné et al. 2015b; Faherty et al. 2016).

As brown dwarfs cool down with time (e.g. Saumon & Marley 2008), their masses cannot be determined from effective temperatures only, and their ages must also be constrained. One of the few methods to precisely constrain the ages of brown dwarfs is to identify those that are members of young stellar associations (e.g. see Zuckerman & Song 2004; Mamajek 2015). Recent efforts have been made to identify such objects at the very-low mass end of the brown dwarf regime, using near-infrared large-area surveys (e.g., Gagné et al. 2015b; Aller et al. 2016; Schneider et al. 2017).

Since objects in the planetary-mass regime are inherently faint, only about a dozen have been discovered yet, most of which still require confirmation from a parallax or radial velocity measurement (e.g., Liu et al. 2013; Gagné et al. 2015a; Schneider et al. 2016; Kellogg et al. 2016).

The Carina-Near moving group was discovered and characterized by Zuckerman et al. (2006). It includes a spatially packed core of eight members and a stream of ten additional probable members more loosely distributed in XYZ Galactic coordinates. Based on a comparison of lithium abundance and X-ray luminosity of the Carina-Near members to those of other associations, Zuckerman et al. (2006) determined an age of 200 ± 50 Myr for the group.

Mamajek (2015) notes that no B- or A-type members of Carina-Near are present in Hipparcos (van Leeuwen 2007), and no systematic survey has been published since Zuckerman et al. (2006) to identify additional low-mass members. The latest-type member of Carina-Near listed by Zuckerman et al. (2006) is the M2.5 dwarf GJ 140 C.

In this paper, we report that the variable T2.5 dwarf SIMP0136+0933 (SIMP J013656.5+093347; Artigau et al. 2006, 2009) is a likely member of Carina-Near. The BASS-Ultracool survey that led to this discovery is summarized in Section 2. New spectroscopic observations are described in Section 3, and the full 6-dimensional kinematics of SIMP0136+0933 are discussed in Section 4. In Section 5, it is demonstrated that SIMP0136+0933 is unlikely a random interloper from the field, and its physical properties are estimated in Section 6. Section 7 discusses the photometric vari-

ability of SIMP0136+0933 in light of its young age. This work is concluded in Section 8.

2. THE BASS-ULTRACOOOL SURVEY

The BANYAN All-Sky Survey-Ultracool (BASS-Ultracool; J. Gagné et al., in preparation) was initiated to locate the late-L to T-type members of young moving groups, with the aim to explore the fundamental properties of isolated planetary-mass objects with cold atmospheres ($T_{\text{eff}} \leq 1500$ K). It relies on a cross-match of large-scale red and near-infrared catalogs such as 2MASS (Skrutskie et al. 2006), AllWISE (Wright et al. 2010), and Pan-STARRS1 (Chambers et al. 2016) to identify high proper motion objects with red $W1 - W2$ AllWISE colors, for which moving group membership is assessed with the Bayesian Analysis for Nearby Young AssociatioNs II tool (BANYAN II; Gagné et al. 2014), and its successor BANYAN Σ (J. Gagné et al., in preparation). First discoveries from this survey include the T5.5 dwarf SDSS J111010.01+011613.1 as a ~ 10 – $12 M_{\text{Jup}}$ member of AB Doradus (Gagné et al. 2015a); 2MASS J09553336–0208403, a young and unusually red L7-type interloper to the TW Hya association (Gagné et al. 2017); and an $\sim L7+T5$ spectral binary candidate member of AB Doradus (D. Bardalez-Gagliuffi et al., submitted to ApJL).

The Zuckerman et al. (2006) list of members and probable members of Carina-Near were cross-matched with the *Gaia* data release 1 (Lindegren et al. 2016), which yielded 12 parallax and proper motion measurements that are more precise than those previously available. New radial velocity measurements from Desidera et al. (2015) were also included for six members. The resulting properties of Carina-Near bona fide members are listed in Table 1.

A multivariate Gaussian model was fit to the resulting kinematics:

$$\mathcal{P}(\bar{x}|\bar{x}_0, \bar{\Sigma}) = \frac{\exp\left(-(\bar{x} - \bar{x}_0)^T \bar{\Sigma}^{-1} (\bar{x} - \bar{x}_0) / 2\right)}{\sqrt{(2\pi)^6 |\bar{\Sigma}|}}, \quad (1)$$

where \bar{x} is a 6-dimensional vector of coordinates in XYZ Galactic coordinates (in pc) and UVW space velocities (in km s^{-1}) in a right-handed system where U points toward the Galactic center, \bar{x}_0 is a 6-dimensional vector representing the center of the group, $\bar{\Sigma}$ is the covariance matrix of all members, and $|\bar{\Sigma}|$ is the determinant of the covariance matrix.

The diagonal elements of $\bar{\Sigma}$ represent variances in the $XYZUVW$ directions, while the off-diagonal elements

Table 1. Updated kinematics of Carina-Near bona fide members.

Name	R.A. (hh:mm:ss.ss)	Decl. (dd:mm:ss.s)	Spectral Type	$\mu_\alpha \cos \delta$ (mas yr ⁻¹)	μ_δ (mas yr ⁻¹)	Rad. velocity (km s ⁻¹)	Parallax (mas)	Ref. ^a
Core Members								
HD 59704	07:29:31.38	-38:07:20.6	F7	-27.32 ± 0.03	68.06 ± 0.04	24.7 ± 1.3	19.24 ± 0.27	1,2,1,3,1
HD 62850	07:42:35.96	-59:17:48.4	G2/3	-53.93 ± 0.07	158.63 ± 0.06	17.1 ± 0.4	30.73 ± 0.22	1,2,1,3,1
HD 62848	07:43:21.40	-52:09:48.5	G0	-56.89 ± 0.03	157.40 ± 0.03	20.5 ± 0.5	29.16 ± 0.56	1,2,1,4,1
HD 63581	07:46:14.70	-59:48:48.4	K0 IV/V	-57.3 ± 0.1	154.6 ± 0.1	18.1 ± 0.1	30.39 ± 0.55	1,5,1,3,1
HD 63608	07:46:16.86	-59:48:31.9	K0	-52.3 ± 0.4	153.2 ± 0.4	16.9 ± 0.3	29.76 ± 0.23	1,2,1,3,1
HR 3070	07:49:12.90	-60:17:01.3	F1	-37.9 ± 0.3	140.3 ± 0.3	16.9 ± 0.4	28.9 ± 0.3	6,2,6,4,6
CPD-52 1153 A	07:20:21.36	-52:18:39.3	F2	-36.88 ± 0.05	146.69 ± 0.05	17.3 ± 1.5	32.75 ± 0.69	1,2,1,7,1
CPD-52 1153 B	07:20:21.81	-52:18:31.2	G0	15.5 ± 3.9	...	1,2,7,
Stream Members								
GJ 140 AB	03:24:06.65	+23:47:06.7	M1+M1	225.3 ± 4.5	-131.4 ± 3.7	19 ± 2	51.3 ± 4.7	1,2,6,2,6
GJ 140 C	03:24:13.08	+23:46:17.4	M2.5	199 ± 8	-112 ± 8	18 ± 3	...	1,2,8,2,
GJ 358	09:39:45.68	-41:03:57.9	M2	-526.6 ± 1.4	356.4 ± 1.4	18 ± 3	105.6 ± 1.6	1,2,6,2,6
HD 108574	12:28:04.19	+44:47:39.4	F7	-181.8 ± 0.1	-4.5 ± 0.1	-2.3 ± 0.3	22.01 ± 0.24	1,2,1,4,1
HD 108575	12:28:04.54	+44:47:30.5	G0	-180.7 ± 0.1	0.5 ± 0.1	-1.3 ± 0.9	21.84 ± 0.24	1,2,1,4,1
HD 103742	11:56:42.11	-32:16:05.5	G3	-172.0 ± 0.4	-8.3 ± 0.3	5.9 ± 0.1	27.97 ± 0.33	1,2,1,3,1
HD 103743	11:56:43.57	-32:16:02.8	G3	-178.8 ± 0.6	-7.1 ± 0.4	6.9 ± 0.5	28.23 ± 0.26	1,2,1,3,1
GJ 900	23:35:00.62	+01:36:19.9	M0	340.9 ± 0.1	27.14 ± 0.08	-9.4 ± 1.1	48.17 ± 0.31	1,2,1,4,1
GJ 907.1	23:48:25.93	-12:59:14.6	K8	230.2 ± 3.3	21.0 ± 2.0	-8.4 ± 0.5	35.46 ± 2.2	1,2,6,9,6

^aAll members were determined by Zuckerman et al. (2006). References for positions, spectral types, proper motions, radial velocities and parallaxes are given in this respective order for each individual object.

References—(1) Lindegren et al. 2016, (2) Zuckerman et al. 2006, (3) Desidera et al. 2015, (4) Gontcharov 2006, (5) Gray et al. 2006, (6) van Leeuwen 2007, (7) Nordström et al. 2004, (8) Zacharias et al. 2013, (9) Torres et al. 2006.

represent correlations between spatial and kinematic coordinates, which can be related to rotation angles in 6-dimensional space. This multivariate model is a generalization of the freely rotating 3D ellipsoid models used in BANYAN II, as it allows for correlations in the spatial and kinematic coordinates. The resulting model parameters are (in order of $XYZUVW$):

$$\bar{x}_0 = \begin{bmatrix} -2.39 & -18.55 & -4.21 & -26.49 & -17.52 & -2.34 \end{bmatrix},$$

$$\bar{\Sigma} = \begin{bmatrix} 60.5 & -16.7 & -15.0 & 3.8 & 2.0 & 6.4 \\ -16.7 & 434.3 & 47.3 & -46.4 & 7.9 & -1.6 \\ -15.0 & 47.3 & 300.1 & -15.7 & -23.1 & -23.4 \\ 3.8 & -46.4 & -15.7 & 10.2 & 0.5 & -0.5 \\ 2.0 & 7.9 & -23.1 & 0.5 & 3.5 & 2.2 \\ 6.4 & -1.6 & -23.4 & -0.5 & 2.2 & 3.8 \end{bmatrix},$$

(2)

in units of pc and km s⁻¹.

In this survey, SIMP0136+0933 was identified as a candidate member of Carina-Near from a cross-match

of 2MASS and AllWISE sources with colors redder than $W1 - W2 = 0.6$, which corresponds to spectral types later than $\sim L8$ (field dwarfs) or $\sim L5$ (young dwarfs; Faherty et al. 2016). This T2.5 dwarf was discovered as part of the SIMP survey (Artigau et al. 2006; Robert et al. 2016) and has been the subject of extensive photometric follow-up due to its photometric variability (e.g., see Artigau et al. 2009; Metchev et al. 2013; Radigan et al. 2014; Croll et al. 2016).

A proper motion derived from 2MASS and AllWISE alone categorized it as a high-probability (>99.9%) candidate member of the Carina-Near moving group using a preliminary version of the BANYAN Σ tool, with a kinematic distance (5.6 ± 0.3 pc) placing it along the sequence of known T dwarfs in near-infrared color-magnitude diagrams. Using the updated astrometry from Weinberger et al. (2016) preserved a high Bayesian membership probability of >99.9%, with a statistical radial velocity prediction of 9.4 ± 0.8 km s⁻¹ if it is a member of Carina-Near.

3. OBSERVATIONS

SIMP0136+0933 was observed with the Near InfraRed Spectrometer (NIRSPEC; McLean et al. 2000) on the Keck II Telescope on 2013 October 16 and 2016 February 2. The first night had moderate cloud coverage with $\sim 60\%$ humidity and a $1''$ seeing, while the second night was clear with a $0''.8$ seeing. The high-dispersion cross-dispersed mode with the NIRSPEC-7 filter and the $0''.432$ -wide slit were used, yielding a resolving power of $\lambda/\Delta\lambda \approx 20,000$ over $2.00\text{--}2.39\ \mu\text{m}$. Two exposures of 900s (2013 October) and 750s (2016 February) were obtained at airmasses of 1.11 and 1.15, yielding signal-to-noise ratios of ~ 20 and ~ 13 per pixel after reduction. The A0V-type standard HD 6457 was observed immediately after SIMP0136+0933 at a similar airmass for telluric correction. A single NeArXeKr calibration lamp exposure and ten 4.4s “on” and “off” flat-field exposures were obtained at the end of each night for wavelength calibration and correction of pixel-to-pixel variations in detector response. The data were reduced with a modified version of the REDSPEC package as described in Burgasser et al. (2015).

4. THE KINEMATICS OF SIMP0136+0933

Spectral data in order 33 ($2.29\text{--}2.33\ \mu\text{m}$) were forward-modeled using the Markov Chain Monte Carlo analysis described in detail in Burgasser et al. (2016). We used the atmosphere models of Allard et al. (2012) and the telluric transmission spectrum from the Solar atlas of Livingston & Wallace (1991). Radial and rotational velocities and their uncertainties were determined by marginalizing over the Markov chains, yielding consistent results between the two epochs (differences of 0.4 and $0.1\ \text{km s}^{-1}$, respectively). Combining these values as an error-weighted average, we determine a radial velocity of $11.5 \pm 0.4\ \text{km s}^{-1}$ and $v \sin i = 50.9 \pm 0.8\ \text{km s}^{-1}$ for SIMP0136+0933.

The XYZ Galactic coordinates and UVW space velocities of SIMP0136+0933 were calculated by adding the radial velocity measurement to the set of kinematic measurements available in the literature in a 10^4 -elements Monte Carlo simulation that assumes Gaussian measurement errors, and are reported in Table 2. These coordinates place SIMP0136+0933 at $20.9 \pm 11.6\ \text{pc}$ and $6.4 \pm 1.6\ \text{km s}^{-1}$ from the core of the Carina-Near multivariate Gaussian model (the largest kinematic deviation occurs in the U direction, see Figure 1). This makes SIMP0136+0933 a likely member of the Carina-Near stream, which is more spatially extended than its core. The second-nearest Carina-Near member to the Sun, the M2 dwarf GJ 358 ($9.5 \pm 0.1\ \text{pc}$; van Leeuwen 2007), is also a member of its stream (Zuckerman et al. 2006). At a distance of $\sim 6.1\ \text{pc}$, SIMP0136+0933 is the near-

Table 2. Properties of SIMP J013656.5+093347

Property	Value	Reference
Position and Kinematics		
R.A.	01:36:56.62	1
Decl.	+09:33:47.3	1
$\mu_\alpha \cos \delta$ (mas yr^{-1})	1222.70 ± 0.78	1
μ_δ (mas yr^{-1})	0.5 ± 1.2	1
RV (km s^{-1})	11.5 ± 0.4	2
Trigonometric distance (pc)	6.139 ± 0.037	1
X (pc)	-2.967 ± 0.018	2
Y (pc)	2.384 ± 0.014	2
Z (pc)	-4.817 ± 0.029	2
U (km s^{-1})	-33.12 ± 0.26	2
V (km s^{-1})	-17.19 ± 0.20	2
W (km s^{-1})	-2.76 ± 0.32	2
Photometric Properties		
i_{AB} (<i>SDSS12</i>)	20.79 ± 0.06	3
z_{AB} (<i>Pan-STARRS1</i>)	17.33 ± 0.02	4 ^a
z_{AB} (<i>SDSS12</i>)	16.55 ± 0.02	3
y_{AB} (<i>Pan-STARRS1</i>)	15.72 ± 0.03	4 ^a
J (<i>2MASS</i>)	13.46 ± 0.03	5
H (<i>UKIDSS</i>)	12.809 ± 0.002	6
K (<i>UKIDSS</i>)	12.585 ± 0.002	6
$W1$ (<i>AllWISE</i>)	11.94 ± 0.02	7
$W2$ (<i>AllWISE</i>)	10.96 ± 0.02	7
$W3$ (<i>AllWISE</i>)	9.74 ± 0.05	7
Spectroscopic Properties		
Spectral type	$T2.5 \pm 0.5$	8
K I at $1.169\ \mu\text{m}$ (\AA)	8.6 ± 1.0	2
K I at $1.177\ \mu\text{m}$ (\AA)	11.7 ± 1.1	2
K I at $1.243\ \mu\text{m}$ (\AA)	5.4 ± 0.3	2
K I at $1.254\ \mu\text{m}$ (\AA)	8.5 ± 0.3	2
Fundamental Properties		
Age (Myr)	200 ± 50	9
Mass (M_{Jup})	12.7 ± 1.0	2
Radius (R_{Jup})	1.22 ± 0.01	2
T_{eff} (K)	1098 ± 6	2
$\log g$	4.31 ± 0.03	2
$\log L_*/L_\odot$	-4.688 ± 0.005	2
Rotation period (h)	2.425 ± 0.003	10 ^b
$v \sin i$ (km s^{-1})	50.9 ± 0.8	2
i ($^\circ$)	$55.9^{+1.6}_{-1.5}$	2

^a Average and standard deviation from five PS1 measurements. The dispersion is larger than quoted uncertainties, likely indicating that variability is also present at red-optical wavelengths.

^b S. Bouchard et al. (in prep.) used an improved method and $\sim 8\ \text{hr}$ of J -band monitoring over 2 nights to improve the previous measurement of 2.3895 ± 0.0005 (Artigau et al. 2009).

References—(1) Weinberger et al. 2016, (2) This work, (3) Alam et al. 2015, (4) Chambers et al. 2016, (5) Skrutskie et al. 2006, (6) Lawrence et al. 2007, (7) Kirkpatrick et al. 2014, (8) Artigau et al. 2006, (9) Zuckerman et al. 2006, (10) S. Bouchard et al., in preparation.

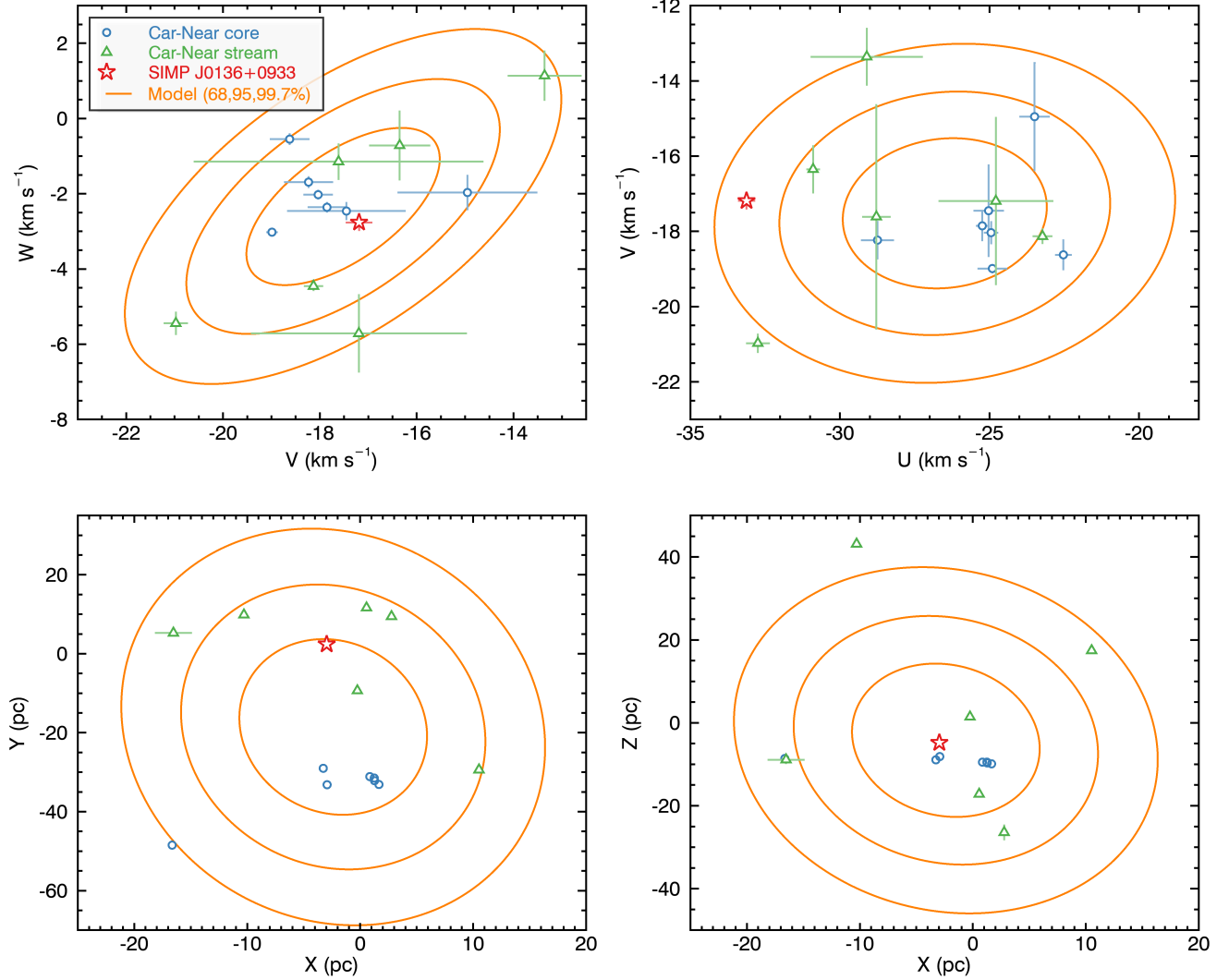


Figure 1. Galactic coordinates XYZ and space velocities UVW of SIMP0136+0933 (red star) compared to bona fide members of the Carina-Near core (blue circles) and stream (green triangles) as defined by Zuckerman et al. (2006), and the multivariate Gaussian model of Carina-Near used in BANYAN Σ (orange lines of 68%, 95% and 99.7% confidence).

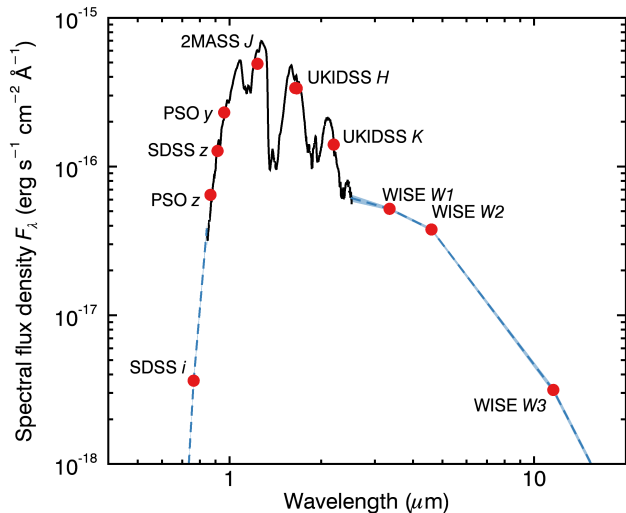


Figure 2. Spectral energy distribution of SIMP0136+0933, built from the GNIRS spectrum of Robert et al. (2016) and optical to infrared photometry listed in Table 2, with the method of Filippazzo et al. (2015).

est known member of any young moving groups, and among the nearest young objects known to date, along with the M4+M5 EQ Peg AB system at 6.18 ± 0.06 pc (van Leeuwen 2007; Zuckerman et al. 2013), the M5 dwarf AP Col at 8.39 ± 0.07 pc (Riedel et al. 2011), and a few possibly young X-ray active mid-M dwarfs from the sample of Riaz et al. (2006; see their Table 4). SIMP0136+0933 is also among the 100 nearest systems to the Sun.

5. FIELD INTERLOPER PROBABILITY

The probability that SIMP0136+0933 is a random field interloper was estimated with the field density of T0–T5 dwarfs measured by Reylé et al. (2010) and a synthetic population of 10^7 objects within 6.14 pc, drawn from the *XYZUVW* distribution of stars in the Galactic neighborhood using the Besançon model (Robin et al. 2012). The separation between each object and the Carina-Near multivariate Gaussian model in *XYZUVW* space was then calculated using the Mahalanobis distance (Mahalanobis 1936), given by:

$$\mathcal{M} = \sqrt{(\bar{x} - \bar{x}_0)^T \bar{\Sigma}^{-1} (\bar{x} - \bar{x}_0)}, \quad (3)$$

where \bar{x} , \bar{x}_0 and $\bar{\Sigma}$ are defined in Section 2. The Mahalanobis distance is a generalized $N\sigma$ distance that accounts for the size and orientation of the multivariate Gaussian model in 6-dimensional space.

A total of 14609 out of 10^7 synthetic objects were found to have a Mahalanobis distance at least as small as that of SIMP0136+0933 ($\mathcal{M} = 3.28$). Adjusting this result to the T0–T5 field density of $2.0^{+0.3}_{-0.2} \cdot$

10^{-3} objects pc^{-3} measured by Reylé et al. (2010), this corresponds to $4.52^{+0.4}_{-0.3} \cdot 10^{-3}$ expected occurrences. Based on Poisson statistics, the detection of at least one early T dwarf such as SIMP0136+0933 thus has a 0.2% probability of being a chance event. This analysis does not assume a young age for SIMP0136+0933.

6. FUNDAMENTAL PROPERTIES

The spectral energy distribution of SIMP0136+0933 was built from a combination of the literature SpeX spectrum (Burgasser et al. 2008) with SDSS, Pan-STARRS1, 2MASS and AllWISE photometry (see Table 2), and is displayed in Figure 2. The method of Filippazzo et al. (2015) was used to perform an empirical measurement of its bolometric luminosity $\log L_*/L_\odot = -4.688 \pm 0.005$, and the Saumon & Marley (2008) models at 200 ± 50 Myr were used to infer a radius of $1.22 \pm 0.01 R_{\text{Jup}}$. These properties were converted to an effective temperature using the Stefan-Boltzmann law, yielding $T_{\text{eff}} = 1098 \pm 6$ K, at the lower-end of T2–T3 field dwarf temperatures (Filippazzo et al. 2015). This is consistent with the observed trend that young brown dwarfs tend to have slightly lower effective temperatures at a given spectral type (Metchev & Hillenbrand 2006; Faherty et al. 2012; Gagné et al. 2015b).

A corresponding mass and surface gravity of $12.7 \pm 1.0 M_{\text{Jup}}$ and $\log g = 4.31 \pm 0.03$ were obtained from the Saumon & Marley (2008) evolutionary models. As displayed in Figure 3(a), a comparison of these values with the models of Allard et al. (2012) implies that SIMP0136+0933 should have burned roughly half of its deuterium content. The bolometric luminosity of SIMP0136+0933 is slightly fainter than average T2.5 dwarfs (Filippazzo et al. 2015) although it is located within the 1σ range of the field distribution. The ~ 150 Myr-old T4.5 dwarf GU Psc b is similarly fainter than the field dwarfs sequence and yields a comparable $\log L_*/L_\odot = 4.87 \pm 0.10$ (Filippazzo et al. 2015).

The $v \sin i$ measurement obtained in Section 4 was combined with the rotation period of Artigau et al. (2009) to constrain the inclination of SIMP0136+0933 to $i = 55.9^{+1.6}_{-1.5}^\circ$, assuming the Saumon & Marley (2008) radius at the age of Carina-Near. Without making any assumption on the age of SIMP0136+0933, the radius of SIMP0136+0933 can be constrained to a lower limit of $1.01 \pm 0.02 R_{\text{Jup}}$, which would correspond to it being observed equator on, or to larger radii at other inclinations. This radius lower limit can be translated to an upper age limit of 910^{+26}_{-110} Myr, or an upper mass limit of $42.6^{+2.5}_{-2.4} M_{\text{Jup}}$, based on the Saumon & Marley (2008) models and the measured bolometric luminosity (see Figure 3(b)). Adding the upper limit of this age

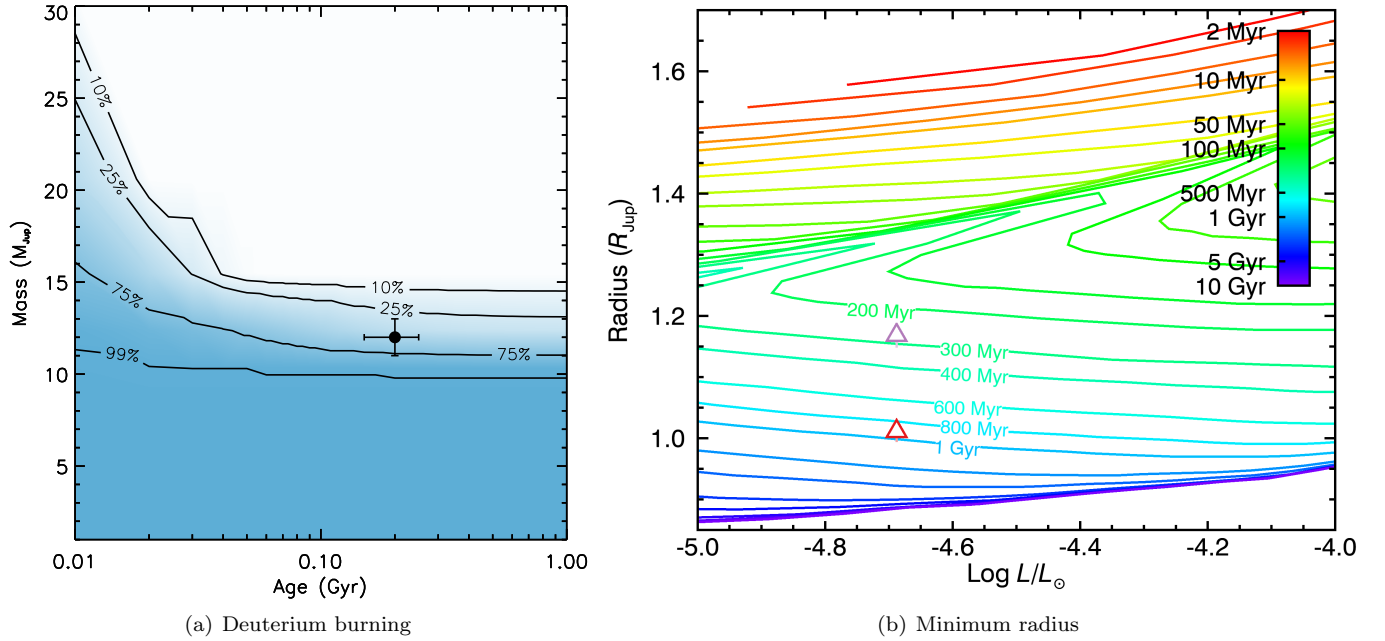


Figure 3. Fundamental properties of SIMP0136+0933. Left panel: deuterium fraction left as a function of age at the brown dwarf/planetary boundary. The models of Allard et al. (2012) at the age and estimated mass of SIMP0136+0933 suggest that it should only have partially depleted its deuterium content. Right panel: minimum radius of SIMP0136+0933 (red triangle) obtained from $v \sin i$ and rotational periods only; and minimum radius when the $i < 60^\circ$ constraint is added (purple triangle); and the models of Saumon & Marley (2008; thick colored lines).

constraint to the analysis presented in Section 5 further reduces the field interloper probability down to 0.0001%.

A preliminary analysis of the harmonics in the long-term light curve of SIMP0136+0933 which assumes that its variability is dominated by a single spot constrains its inclination to $i < 60^\circ$ (S. Bouchard et al., in preparation). If the single-spot hypothesis can be confirmed, it will further constrain the radius to values larger than $1.17 \pm 0.02 R_{\text{Jup}}$, and a model-dependent age below 280_{-30}^{+40} Myr, which would corroborate the Carina-Near membership and the planetary mass of SIMP0136+0933.

The method of McLean et al. (2003) was used to measure K I equivalent widths of 8.6 ± 1.0 , 11.7 ± 1.1 , 5.4 ± 0.3 , and $8.5 \pm 0.3 \text{ \AA}$ (at 1.169, 1.177, 1.243, and 1.254 μm , respectively) from the GNIRS spectrum. These values are consistent with the field population of T2–T3 dwarfs (McLean et al. 2003), which is not unexpected given that the slightly younger T5.5 dwarf SDSS J111010.01+011613.1 (~ 150 Myr; Gagné et al. 2015a) has K I equivalent widths consistent or slightly weaker than those of field T5 dwarfs (Martin et al. 2017).

7. VARIABILITY AND AGE

Surface gravity is a key parameter in the description of dust behavior in brown dwarf atmospheres. Among L dwarfs, thicker cloud decks are expected

among lower gravity objects due to the slower settling rates. Thick cloud decks lead to a redistribution of the near-infrared spectral energy distribution to longer wavelengths, leading to redder infrared colors for low gravity, young objects (Faherty et al. 2016). As dust-bearing clouds of varying thicknesses are generally invoked to explain such variability, a gravity-dependence of variability behavior can be expected. Metchev et al. (2015) included a sample of low-gravity L dwarfs in the large SPITZER sample of photometric observations, and found tentative indications that the low-gravity objects displayed larger photometric amplitudes even though the fraction of variable objects appeared to be independent of surface gravity. The detection of large (7–10%) photometric J -band variability in very-low gravity L dwarfs (PSO J318.5338–22.8603, WISEP J004701.06+680352.1; Biller et al. 2015; Lew et al. 2016) appears to corroborate these findings, as earlier surveys at these wavelengths failed to uncover $> 4\%$ variability among L dwarfs.

Figure 4 compiles J , 3.6 μm and 4.5 μm variability detections in a spectral-type versus color diagram. The detections to date suggest a higher fraction of high-amplitude variables among very red L-type dwarfs, but some of these discoveries were made from surveys explicitly targeting red, low-gravity objects. Overall, this tentative correlation between surface gravity and vari-

ability amplitude has yet to be set on firm statistical grounds.

Whether low-gravity T dwarfs exhibit stronger variability remains unknown, but SIMP0136+0933 may provide the first such example with its $\sim 1\text{--}6\%$ J -band variability (Croll et al. 2016). Only a handful of low-gravity T dwarfs are currently confirmed (e.g., Gagné et al. 2015a; Naud et al. 2014), none of which have reported measurements assessing their photometric variability.

8. SUMMARY AND CONCLUSIONS

This paper presents the discovery that the nearby (~ 6 pc) T2.5 dwarf SIMP0136+0933 is a likely member of the 200 Myr-old Carina-Near moving group, based on the new Bayesian analysis tool BANYAN Σ and radial velocity measurement. At this young age, SIMP0136+0933 has a model-dependent mass of $12.7 \pm 1.0 M_{\text{Jup}}$ at the planetary-mass boundary. Given the tentative correlation between high-amplitude variability and youth in L dwarfs, the discovery that SIMP0136+0933 is a member of Carina-Near indicates that such a correlation could hold in the T dwarfs regime, however more young T dwarfs will need to be investigated for variability to verify this. SIMP0136+0933 is an even more powerful benchmark than previously appreciated and will help to understand weather patterns in gaseous giant atmospheres.

The authors would like to thank the anonymous referee for useful comments and suggestions. This work was supported in part through grants from the Natural Science and Engineering Research Council of Canada. This research made use of: data products from the *Wide-field Infrared Survey Explorer* (WISE; Wright et al. 2010), which is a joint project of the University of California, Los Angeles, and the

Jet Propulsion Laboratory at the California Institute of Technology (Caltech), funded by NASA, and of data from the European Space Agency (ESA) mission *Gaia* (<http://www.cosmos.esa.int/gaia>), processed by the *Gaia* Data Processing and Analysis Consortium (DPAC, <http://www.cosmos.esa.int/web/gaia/dpac/consortium>). The data presented herein were obtained at the W.M. Keck Observatory, which is operated as a scientific partnership among Caltech, the University of California and NASA. The Observatory was made possible by the generous financial support of the W.M. Keck Foundation. The authors wish to recognize and acknowledge the very significant cultural role and reverence that the summit of Mauna Kea has always had within the indigenous Hawaiian community. We are most fortunate to have the opportunity to conduct observations from this mountain.

JG wrote most of the manuscript, generated Figures 1, 2 and 3(b), led the BASS-Ultracool survey and the development of the BANYAN Σ tool, and the kinematic analysis; *JKF* led the spectral energy distribution analysis. *AJB* acquired and reduced the NIRSPEC spectrum and measured the radial velocity and $v \sin i$. *ÉA* wrote Section 7 and generated Figures 3(a) and 4. *SB* provided useful discussions on the photometric properties of SIMP0136+0933 and unpublished photometric data. *LA* cross-matched SIMP0136+0933 with individual epochs of the Pan-STARRS1 catalog. *RD* and *DL* participated in the development of the BANYAN Σ tool. *DCBG* observed the NIRSPEC spectrum.

Facility: Keck:II (NIRSPEC)

Software: BANYAN Σ , BANYAN II, Python, IDL by Harris Geospatial, Overleaf

REFERENCES

- Alam, S., Albareti, F. D., Allende Prieto, C., et al. 2015, *The Astrophysical Journal Supplement Series*, 219, 12
- Allard, F., Homeier, D., & Freytag, B. 2012, *Philosophical Transactions of the Royal Society A: Mathematical*, 370, 2765
- Aller, K. M., Liu, M. C., Magnier, E. A., et al. 2016, *The Astrophysical Journal*, 821, 120
- Artigau, É., Bouchard, S., Doyon, R., & Lafrenière, D. 2009, *The Astrophysical Journal*, 701, 1534
- Artigau, É., Doyon, R., Lafrenière, D., et al. 2006, *The Astrophysical Journal*, 651, L57
- Billar, B. A., Vos, J., Bonavita, M., et al. 2015, *The Astrophysical Journal Letters*, 813, L23
- Burgasser, A. J., Blake, C. H., Gelino, C. R., Sahlmann, J., & Bardalez Gagliuffi, D. 2016, *The Astrophysical Journal*, 827, 25
- Burgasser, A. J., Liu, M. C., Ireland, M. J., Cruz, K. L., & Dupuy, T. J. 2008, *The Astrophysical Journal*, 681, 579
- Burgasser, A. J., Gillon, M., Melis, C., et al. 2015, *The Astronomical Journal*, 149, 104
- Chambers, K. C., Magnier, E. A., Metcalfe, N., et al. 2016, arXiv.org, arXiv:1612.05560

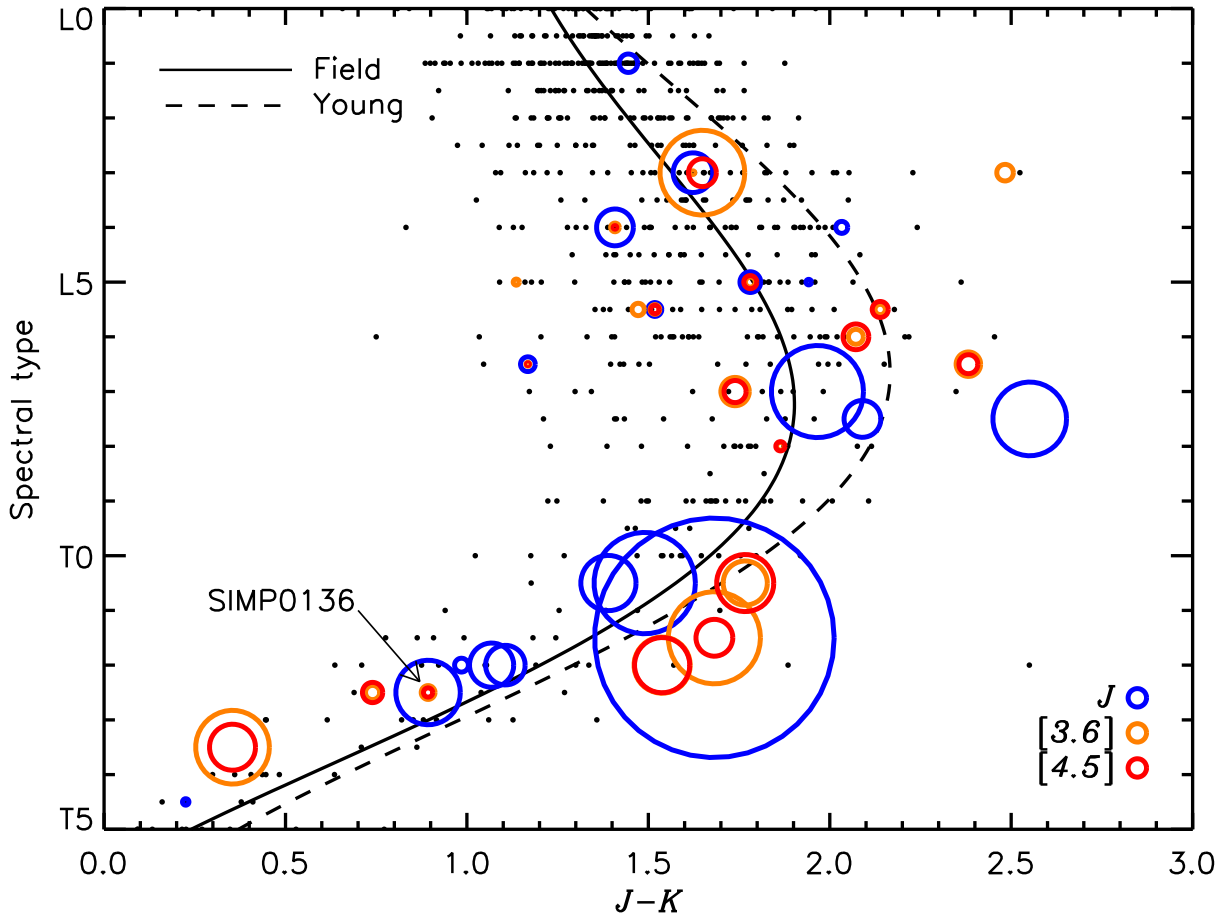


Figure 4. Brown dwarfs with detected photometric variability as a function of spectral type and near-infrared colors. The colors of individual circles indicate the wavelength where variability is detected, and the size of the circle indicates the variability amplitude in linear scale. The polynomial relations of Faherty et al. (2016) for field and young brown dwarfs are displayed as solid and dashed lines, respectively. In the L spectral class, there is tentative evidence for high-amplitude variable brown dwarfs to be more frequent at redder near-infrared colors (Metchev et al. 2015), which are generally associated with younger, low-gravity brown dwarfs. This figure was built with data from Dupuy & Liu (2012), Radigan (2014) and references therein.

Croll, B., Muirhead, P. S., Lichtman, J., et al. 2016, arXiv.org, arXiv:1609.03587

Desidera, S., Covino, E., Messina, S., et al. 2015, *Astronomy & Astrophysics*, 573, A126

Dupuy, T. J., & Liu, M. C. 2012, *The Astrophysical Journal Supplement*, 201, 19

Faherty, J. K., Burgasser, A. J., Walter, F. M., et al. 2012, *The Astrophysical Journal*, 752, 56

Faherty, J. K., Riedel, A. R., Cruz, K. L., et al. 2016, *The Astrophysical Journal Supplement Series*, 225, 10

Filippazzo, J. C., Rice, E. L., Faherty, J., et al. 2015, *The Astrophysical Journal*, 810, 158

Gagné, J., Burgasser, A. J., Faherty, J. K., et al. 2015a, *The Astrophysical Journal Letters*, 808, L20

Gagné, J., Lafrenière, D., Doyon, R., Malo, L., & Artigau, É. 2014, *The Astrophysical Journal*, 783, 121

Gagné, J., Faherty, J. K., Cruz, K. L., et al. 2015b, *The Astrophysical Journal Supplement Series*, 219, 33

Gagné, J., Faherty, J. K., Mamajek, E. E., et al. 2017, *The Astrophysical Journal Supplement Series*, 228, 18

Gontcharov, G. A. 2006, *Astronomy Letters*, 32, 759

Gray, R. O., Corbally, C. J., Garrison, R. F., et al. 2006, *The Astronomical Journal*, 132, 161

Kellogg, K., Metchev, S., Gagné, J., & Faherty, J. 2016, *The Astrophysical Journal Letters*, 821, L15

Kirkpatrick, J. D., Schneider, A., Fajardo-Acosta, S., et al. 2014, *The Astrophysical Journal*, 783, 122

Lawrence, A., Warren, S. J., Almaini, O., et al. 2007, *Monthly Notices of the Royal Astronomical Society*, 379, 1599

Lew, B. W. P., Apai, D., Zhou, Y., et al. 2016, *The Astrophysical Journal Letters*, 829, L32

Lindgren, L., Lammers, U., Bastian, U., et al. 2016, *Astronomy & Astrophysics*, 595, A4

Liu, M. C., Magnier, E. A., Deacon, N. R., et al. 2013, *The Astrophysical Journal Letters*, 777, L20

- Livingston, W., & Wallace, L. 1991, NSO Technical Report
- Mahalanobis, P. C. 1936, . . . National Institute of Science of India
- Mamajek, E. E. 2015, *Young Stars & Planets Near the Sun*, 314, 21
- Martin, E. C., Mace, G. N., McLean, I. S., et al. 2017, *The Astrophysical Journal*, 838, 73
- McLean, I. S., Graham, J. R., Becklin, E. E., et al. 2000, *Proc. SPIE Vol. 4008*, 4008, 1048
- McLean, I. S., McGovern, M. R., Burgasser, A. J., et al. 2003, *The Astrophysical Journal*, 596, 561
- Metchev, S., Apai, D., Radigan, J., et al. 2013, *Astronomische Nachrichten*, 334, 40
- Metchev, S. A., & Hillenbrand, L. A. 2006, *The Astrophysical Journal*, 651, 1166
- Metchev, S. A., Heinze, A., Apai, D., et al. 2015, *The Astrophysical Journal*, 799, 154
- Naud, M.-È., Artigau, É., Malo, L., et al. 2014, *The Astrophysical Journal*, 787, 5
- Nordström, B., Mayor, M., Andersen, J., et al. 2004, *Astronomy & Astrophysics*, 418, 989
- Radigan, J. 2014, *The Astrophysical Journal*, 797, 120
- Radigan, J., Lafrenière, D., Jayawardhana, R., & Artigau, É. 2014, *The Astrophysical Journal*, 793, 75
- Reylé, C., Delorme, P., Willott, C. J., et al. 2010, *Astronomy & Astrophysics*, 522, A112
- Riaz, B., Gizis, J. E., & Harvin, J. 2006, *The Astronomical Journal*, 132, 866
- Riedel, A. R., Murphy, S. J., Henry, T. J., et al. 2011, *The Astronomical Journal*, 142, 104
- Robert, J., Gagné, J., Artigau, É., et al. 2016, *The Astrophysical Journal*, 830, 144
- Robin, A. C., Marshall, D. J., Schultheis, M., & Reylé, C. 2012, *Astronomy & Astrophysics*, 538, A106
- Saumon, D., & Marley, M. S. 2008, *The Astrophysical Journal*, 689, 1327
- Schneider, A. C., Windsor, J., Cushing, M. C., & Kirkpatrick, J. D. 2017, arXiv.org, arXiv:1703.03774
- Schneider, A. C., Windsor, J., Cushing, M. C., Kirkpatrick, J. D., & Wright, E. L. 2016, *The Astrophysical Journal Letters*, 822, L1
- Skrutskie, M. F., Cutri, R. M., Stiening, R., et al. 2006, *The Astronomical Journal*, 131, 1163
- Torres, C. A. O., Quast, G. R., da Silva, L., et al. 2006, *Astronomy & Astrophysics*, 460, 695
- van Leeuwen, F. 2007, *Astronomy & Astrophysics*, 474, 653
- Weinberger, A. J., Boss, A. P., Keiser, S. A., et al. 2016, *The Astronomical Journal*, 152, 24
- Wright, E. L., Eisenhardt, P. R. M., Mainzer, A. K., et al. 2010, *The Astronomical Journal*, 140, 1868
- Zacharias, N., Finch, C. T., Girard, T. M., et al. 2013, *The Astronomical Journal*, 145, 44
- Zuckerman, B., Bessell, M. S., Song, I., & Kim, S. 2006, *The Astrophysical Journal*, 649, L115
- Zuckerman, B., & Song, I. 2004, *Annual Review of Astronomy & Astrophysics*, 42, 685
- Zuckerman, B., Vican, L., Song, I., & Schneider, A. 2013, *The Astrophysical Journal*, 778, 5